

See discussions, stats, and author profiles for this publication at: <https://www.researchgate.net/publication/7911132>

Complexes of DNA Bases and Gold Clusters Au₃ and Au₄ Involving Nonconventional N–H···Au Hydrogen Bonding

ARTICLE *in* NANO LETTERS · MAY 2005

Impact Factor: 13.59 · DOI: 10.1021/nl050194m · Source: PubMed

CITATIONS

78

READS

40

2 AUTHORS:



Eugene S Kryachko

University of Liège

139 PUBLICATIONS 2,016 CITATIONS

SEE PROFILE



F. Remacle

University of Liège

185 PUBLICATIONS 3,524 CITATIONS

SEE PROFILE

Complexes of DNA Bases and Gold Clusters Au_3 and Au_4 Involving Nonconventional $\text{N-H}\cdots\text{Au}$ Hydrogen Bonding

E. S. Kryachko^{*,†} and F. Remacle^{*,‡}

Department of Chemistry, B6c, Université de Liège, B-4000 Liège, Belgium, and Bogoliubov Institute for Theoretical Physics, Kiev, 03143 Ukraine

Received January 31, 2005

ABSTRACT

DNA base-gold interactions are studied theoretically at the DFT level using Au_3 and Au_4 clusters as simple catalytic models for Au particles. The bonding between DNA bases and gold clusters occurs via the anchoring of a Au atom to the N or O atoms of the bases. In the most stable planar base- Au_3 complexes, the Au–N or Au–O anchor bonds are reinforced by $\text{N-H}\cdots\text{Au}$ bonds. The mechanism of formation of these nonconventional H-bonds is discussed.

DNA–gold interactions play an important role in nano- and biotechnology (see refs 1–5 and references therein). Recent experimental studies have shown that the DNA bases adenine (A), thymine (T), guanine (G), and cytosine (C) interact with Au surfaces and Au clusters and adsorb at Au electrodes in a complex and sequence-dependent manner.^{4,5} Their relative affinities to adsorb on polycrystalline Au films are ordered as $\text{A} > \text{C} \geq \text{G} > \text{T}$.^{4a} Mirkin and co-workers^{4b} have recently reported that the heats of desorption of the nucleic acid bases from Au thin films vary within 26.3–34.9 kcal mol^{−1} and obey the following order: $\text{G} > \text{A} \geq \text{C} > \text{T}$. Chen et al.^{4d} and Giese and McNaughton^{4e} have suggested that adenine binds Au via the N_6 exocyclic amino group and the N_7 atom. However, the mechanism of binding of DNA bases with gold as well as the precise geometries of their complexes remain still unknown. These issues are addressed in the present work.

We investigate theoretically the interaction of DNA bases with bare Au_3 and Au_4 gold clusters as simple catalytic models of Au particles,⁶ using the density functional B3LYP potential together with the energy-consistent 19-valence electron relativistic effective core potential for gold developed by Ermler, Christiansen, and co-workers⁷ (see also ref 8 for current work and references therein) and the 6-31+G(d) basis set for DNA bases, as they are implemented in the GAUSSIAN 03 package of quantum chemical programs.⁹ All geometrical optimizations use the keywords “tight” and

“Int=UltraFine”. The harmonic vibrational frequencies, zero-point vibrational energies (ZPVE), and enthalpies were also calculated. The reported binding energies include the ZPVE correction. To assess basis-set effects, some selected DNA–base–gold structures were further studied at the B3LYP/RECP (gold) \cup 6-31++G(d,p) (DNA base) computational level.

Single gold atom–DNA base complexes are characterized by very low binding energies: adenine (2.2–2.5 kcal mol^{−1}), guanine (0.8 kcal mol^{−1}), and cytosine (1.2 and 3.8 kcal mol^{−1}), whereas no stable complex is formed with thymine. On the other hand, the binding energy of a bare Au_3 gold cluster to DNA bases (see Table 1) is about an order of magnitude higher. The most stable base– Au_3 complexes are planar and formed either via Au–N or Au–O coordinative (“anchor”) bonds (Figures 1–4). The Au_3 cluster preferentially binds adenine at N_1 , N_3 , and N_7 (Figure 1), thymine at O_2 and O_4 (Figure 2), guanine at the N_3 , O_6 , and N_7 atoms (Figure 3), and cytosine at O_2 and N_3 (Figure 4). The binding energies are larger (they fall within the interval of 20.7–25.4 kcal mol^{−1}), for complexes with a Au–N anchor bond than for complexes with a Au–O bond (for the latter, $E_b \in 10.5$ –20.0 kcal mol^{−1}), indicating that the Au–N bonding is stronger. Correspondingly, the Au–N bonds are also shorter, ranging from 2.130 to 2.153 Å, compared to the Au–O bonds (2.177–2.239 Å). The most stable complex has a binding energy $E_b = 25.4$ kcal mol^{−1} and is formed between cytosine and Au_3 anchored to the N_3 atom on the N_2 side. The complexes $\text{A}\cdot\text{Au}_3$, $\text{G}\cdot\text{Au}_3$, and $\text{C}\cdot\text{Au}_3$ with the Au_3 –amino nitrogen bonding (also shown in Figures 1, 3,

* Corresponding authors. E-mail: eugene.kryachko@ulg.ac.be; fremacle@ulg.ac.be.

[†] Université de Liège and Bogoliubov Institute for Theoretical Physics.

[‡] Maître de Recherches, FNRS (Université de Liège, Belgium).

Table 1. Some Key Features of the Planar DNA-base–Au₃ Complexes with the N–H···Au H-Bond^a

complex	E_b	$-\Delta H_f$	anchor bond	$\Delta R(\text{N–H})$	$r(\text{H}\cdots\text{Au})$	$\angle \text{N–H}\cdots\text{Au}$	$\Delta\nu(\text{N–H})$	R_{IR}	$\delta\sigma_{\text{iso}}$	$\delta\sigma_{\text{an}}$
A·Au ₃ (N ₁)	22.6	22.7	2.153	0.009	2.836	175.2	153	5.6	–2.4	10.3
A·Au ₃ (N ₃)	24.4	24.0	2.138	0.014	2.698	160.8	252	8.7	–2.4	13.0
	(24.0)			(0.007)			(270)			
A·Au ₃ (N ₇)	22.3	21.9	2.130	0.007	2.816	165.1	116	9.0	–2.2	14.0
T·Au ₃ (O ₂ ; N ₁ side)	14.4	13.9	2.218	0.017	2.608	178.8	324	11.0	–2.9	16.6
T·Au ₃ (O ₂ ; N ₃ side)	10.8	10.3	2.227	0.011	2.913	171.8	199	9.0	–1.9	13.9
T·Au ₃ (O ₄)	12.4	11.9	2.209	0.013	2.883	174.4	224	9.0	–2.2	14.1
G·Au ₃ (N ₃ ; N ₂ side)	20.7	20.1	2.147	0.009	2.890	176.1	115	9.0	–2.5	10.2
G·Au ₃ (N ₃ ; N ₉ side)	20.9	20.3	2.146	0.010	2.841	161.8	181	6.0	–1.8	11.7
G·Au ₃ (O ₆ ; N ₁ side)	18.4	17.9	2.186	0.015	2.580	173.1	302	15.0	–3.2	18.7
	(18.4)			(0.012)			(324)			
C·Au ₃ (O ₂ ; N ₁ side)	20.0	19.5	2.177	0.016	2.627	178.9	306	14.0	–3.2	17.6
C·Au ₃ (N ₃)	25.4	25.1	2.164	0.014	2.673	179.7	232	8.0	–3.2	12.6

^a Three H···Au bond lengths, $r(\text{H}_3\cdots\text{Au}_8) = 2.883$ Å in T·Au₃(O₄), $r(\text{H}_2'\cdots\text{Au}_{11}) = 2.890$ Å in G·Au₃(N₃; N₂ side), and $r(\text{H}_3\cdots\text{Au}_8) = 2.913$ Å in T·Au₃(O₂; N₃ side) slightly exceed the sum of van der Waals radii (see also ref 10f and comment (ref 21) therein about an extension of the van der Waals cutoff to 3.0–3.2 Å). The binding energy E_b (including zero-point vibrational energy) and the enthalpy of formation, $-\Delta H_f$, are given in kcal·mol^{–1} and defined with respect to the infinitely separated base and Au₃ cluster. $\Delta\nu(\text{N–H})$ is in cm^{–1}. R_{IR} is the ratio of the IR activities of the corresponding N–H stretches in the H-bonds and in the bases. $\delta\sigma_{\text{iso}}$ and $\delta\sigma_{\text{an}}$ are the NMR shifts (in ppm) taken with respect to the corresponding monomers. The data in parentheses refer to the level B3LYP/RECP (gold) ∪ 6-31++G(d,p) (DNA base). Bond lengths are given in Å and angles in deg.

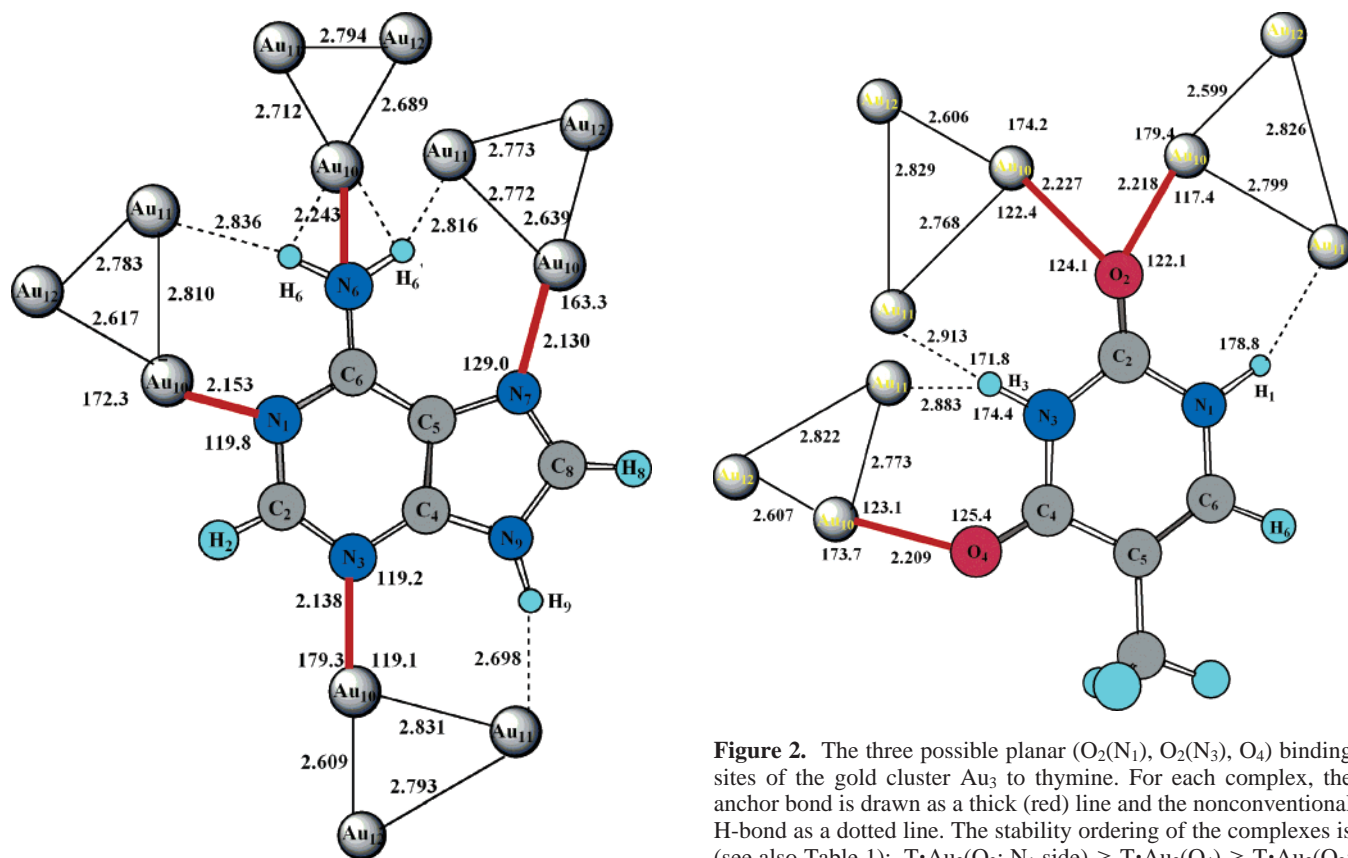


Figure 1. The four possible planar (N₁, N₃, N₇) and nonplanar (N₆) binding sites of the gold cluster Au₃ to adenine. Also shown is the NH₂ anchored complex A·Au₃(N₆). For each complex, the anchor bond is drawn as a thick (red) line and the nonconventional H-bond as a dotted line. The stability ordering of the complexes is (see also Table 1): A·Au₃(N₃) > A·Au₃(N₁) > A·Au₃(N₇) > A·Au₃(N₆). The bond lengths are given in Å and bond angles in deg.

and 4) are nonplanar and less stable, viz., $E_b(\text{A}\cdot\text{Au}_3(\text{N}_6)) = 14.5$, $E_b(\text{G}\cdot\text{Au}_3(\text{N}_2)) = 9.1$, and $E_b(\text{C}\cdot\text{Au}_3(\text{N}_4)) = 11.2$ kcal mol^{–1}. In agreement with the experiments by Lindsay and co-workers^{1a} (see also ref 4g), the complexes between T and

Au₃ anchored to the N₁ and N₃ atoms are unstable. A comparison of the binding energies of planar and nonplanar base–Au₃ complexes leads to the following order for the affinities of the DNA bases to Au₃: C > A > G > T. Since the purines A and G possess four and six anchoring sites for Au₃, respectively, and the pyrimidines C and T have only three, the mean values of the binding energies, averaged over the number of sites, are reordered as A > C > G > T.

The binding energies of the most stable base–Au₃ complexes and their anchor bond lengths are not fully

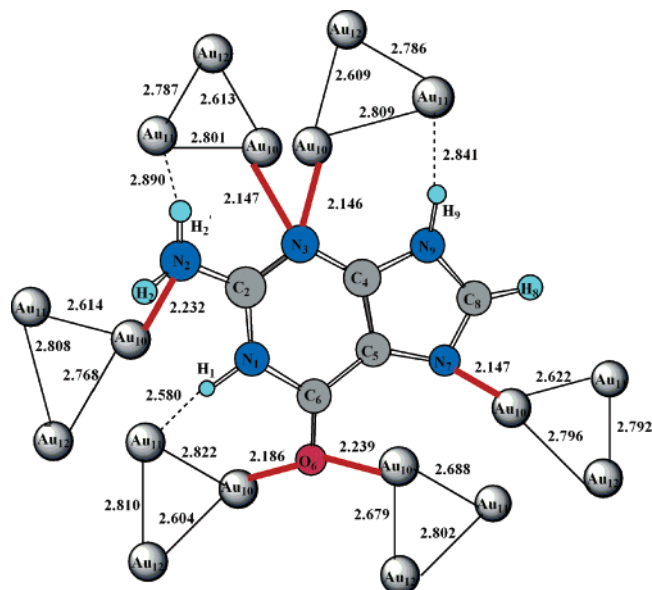


Figure 3. The six possible planar ($N_3(N_2)$, $N_3(N_9)$, $O_6(N_1)$, $O_6(N_7)$, N_7) and nonplanar(N_2) binding sites of the gold cluster Au_3 to guanine. For each complex, the anchor bond is drawn as a thick (red) line and the nonconventional H-bond as a dotted line. The anchoring in N_2 is to the amino group. The stability ordering of the complexes is (see also Table 1): $G \cdot Au_3(N_3; N_9 \text{ side}) > G \cdot Au_3(N_3; N_2 \text{ side}) > G \cdot Au_3(N_7) > G \cdot Au_3(O_6; N_1 \text{ side}) > G \cdot Au_3(O_6; N_7 \text{ side}) > G \cdot Au_3(N_2)$. The bond lengths are given in Å and bond angles in deg.

correlated (see Table 1). For example, the most stable complex $C \cdot Au_3(N_3)$ shown in Figure 4 has a $Au-N$ anchor bond of 2.164 Å, whereas the shortest one, 2.130 Å, is found in $A \cdot Au_3(N_7)$, whose $E_b = 22.3 \text{ kcal mol}^{-1}$. The reason is that the anchor bonds in all reported planar base- Au_3 complexes, except $G \cdot Au_3(N_7)$, are reinforced by the $N-H \cdots Au$ bonds. Note that a similar bonding may also occur between the amino groups and Au_3 in the complexes $A \cdot Au_3(N_6)$, $G \cdot Au_3(N_2)$, and $C \cdot Au_3(N_4)$ (see Figures 1, 3, and 4), but these bonds are much weaker since their corresponding bond angles $\angle NHAu \approx 100^\circ$. Regarding the aforementioned complex $G \cdot Au_3(N_7)$, an extremely weak, $C_8-H_8 \cdots Au_{11}$, bond may also be formed therein due to the very weak proton donor ability of the C_8-H_8 group.^{10c}

The non conventional $N-H \cdots Au$ bonds that are present in the most stable complexes are similar to conventional weak hydrogen bonds since they obey all the necessary prerequisites (see ref 10 and references therein) of the conventional ones, viz.: (i) there exists an evidence of the bond formation; (ii) there exists an evidence that this bond specifically involves a hydrogen atom which is bonded to Au predominantly along the $N-H$ bond direction; (iii) the $N-H$ bond elongates relative to that in the monomer; (iv) there exists a van der Waals cutoff: the hydrogen bond separation $r(H \cdots Au)$ is shorter than the sum of van der Waals radii of H and Au (2.86 Å); (v) the stretching mode $\nu(N-H)$ undergoes a red shift with respect to that in the isolated base and its IR intensity increases; and finally, (vi) proton nuclear magnetic resonance (1H NMR) chemical shifts in the $N-H \cdots Au$ hydrogen bond are shifted downfield compared to the monomer.¹¹ The key features of the $N-H \cdots Au$ bonds of the

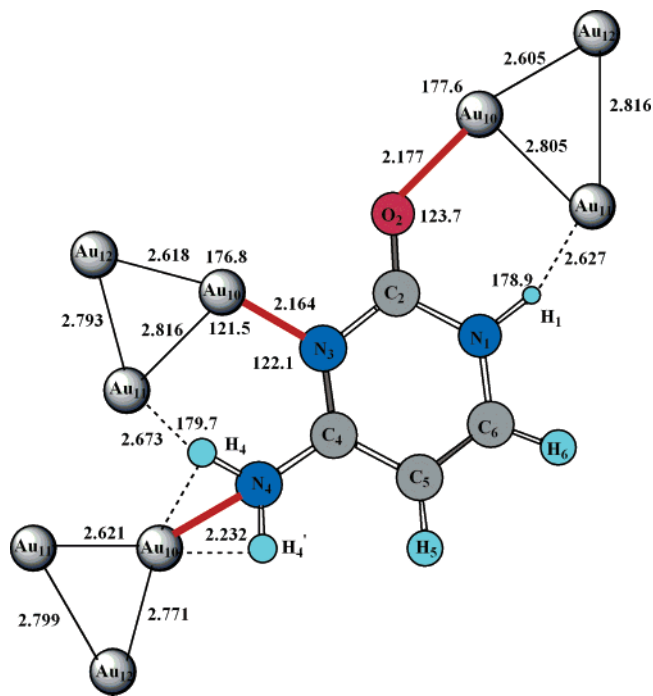


Figure 4. The three possible planar ($O_2(N_1)$, N_3) and nonplanar (N_4) binding sites of the gold cluster Au_3 to cytosine. For each complex, the anchor bond is drawn as a thick (red) line and the nonconventional H-bonds in dotted lines. For the binding site N_4 , the anchor bond is to the NH_2 group. The stability ordering of the complexes is (see also Table 1): $C \cdot Au_3(N_3) > C \cdot Au_3(O_2; N_1 \text{ side}) > C \cdot Au_3(N_4)$. The bond lengths are given in Å and bond angles in deg.

planar base- Au_3 complexes that are gathered in Table 1 demonstrate that these bonds satisfy all the conditions i-vi. Therefore, they can be treated as the nonconventional hydrogen bonds, by analogy with other nonconventional hydrogen bonds with transition metals.¹²

Let us now focus on some specific features of these bonds. Among all the studied complexes $A \cdot Au_3$, the largest red shift of the $\nu(N_9-H_9)$ stretch (252 cm^{-1}) is predicted for the hydrogen bond $N_9-H_9 \cdots Au_{11}$ in $A \cdot Au_3(N_3)$ (see Figure 1). This can be understood from the fact that the N_9-H_9 bond of A is characterized by the smallest deprotonation energy (enthalpy) compared to the other $N-H$ bonds, viz., $DPE(N_9-H_9) = 336.8 \text{ kcal mol}^{-1} < DPE(N_6-H_6') = 355.2 \text{ kcal mol}^{-1} < DPE(N_6-H_6) = 355.8 \text{ kcal mol}^{-1}$,¹³ and, therefore, it is more strongly perturbed by the Au_3 cluster than the amino protons. The three shortest $N-H \cdots Au$ H-bonds (2.580–2.627 Å) are found in the complexes $G \cdot Au_3(O_6; N_1 \text{ side})$, $T \cdot Au_3(O_2; N_1 \text{ side})$, and $C \cdot Au_3(O_2; N_1 \text{ side})$. The corresponding $N-H$ stretching modes are characterized by the largest red shifts (302, 324, and 306 cm^{-1}), the largest IR enhancement factors (15, 11 and 14), and the largest displacements, 0.014–0.017 Å, of the bridging proton toward the gold atom acting as a nonconventional proton acceptor. The high stabilization of these hydrogen bonds is explained by the small deprotonation energies of the involved $N-H$ groups: $DPE(N_1-H_1; G) = 338.4 \text{ kcal mol}^{-1}$, $DPE(N_1-H_1; T) = 334.2 \text{ kcal mol}^{-1} < DPE(N_3-H_3; T) = 346.6 \text{ kcal mol}^{-1}$, and $DPE(N_1-H_1; C) = 345.2 \text{ kcal mol}^{-1} < DPE(N_4-H_4; C) = 354.2 \text{ kcal mol}^{-1}$.¹³ The former inequality also

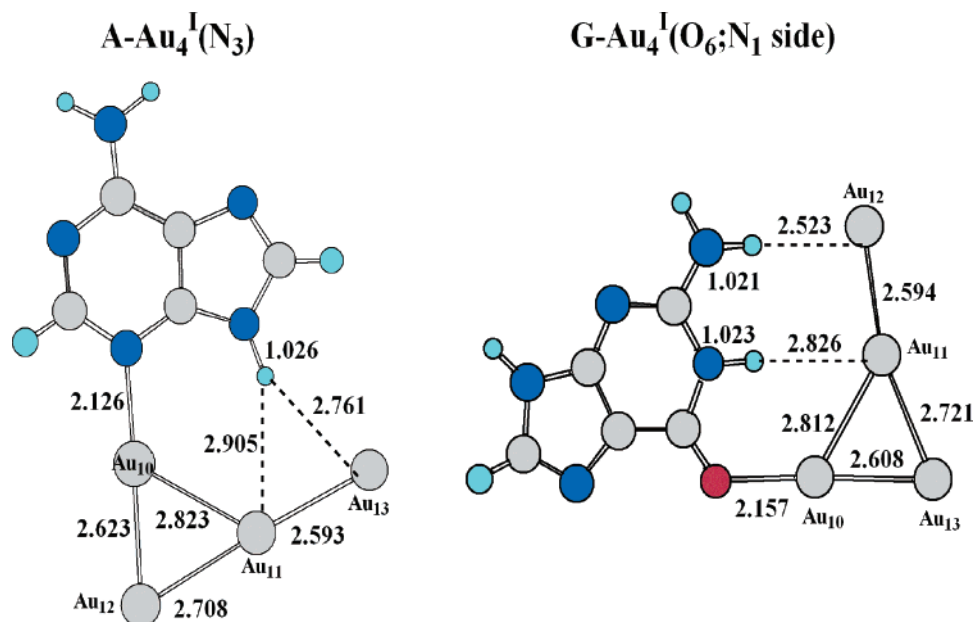


Figure 5. Complexes A·Au₄^I(N₃) and G·Au₄^I(O₆; N₁ side) with a T-shape four-gold cluster. The bond lengths are given in Å and bond angles in deg. Atomic numbering is indicated in Figures 1 and 3. The H-bonds are drawn in dotted lines.

partly explains the difference of 3.6 kcal mol⁻¹ in the binding energies of the complexes T·Au₃(O₂; N₁ side) and T·Au₃(O₂; N₃ side) (see Figure 2) that exhibit quite similar anchor bonds Au₇–O₂. We also notice that the difference in the deprotonation energies of the N₉–H₉ and N₂–H₂' groups of G, viz., DPE(N₉–H₉) = 336.4 kcal mol⁻¹ < DPE(N₂–H₂') = 343.0 kcal mol⁻¹,¹³ explains the difference between the hydrogen bonds N₉–H₉···Au₁₁ and N₂–H₂'···Au₁₁ in the complexes G·Au₃(N₃; N₂ side) and G·Au₃(N₃; N₉ side) (see Figure 3).

The changes in the NMR chemical shift $\delta\sigma_{\text{iso}}(\text{H})$ (prerequisite vi) of the bridging proton in the studied N–H···Au H-bonds are all negative and fall within a narrow interval of –1.8 to –3.2 ppm that is close to $\delta\sigma_{\text{iso}}(\text{H}) = -2.8$ ppm of the water dimer.^{11c} This implies that the base–gold interaction induces a deshielding of the bridging proton. The range of the anisotropic shifts $\delta\sigma_{\text{an}}(\text{H})$ is much wider, from 10.2 to 18.7 ppm, and is also rather close to that of the water dimer.^{11c} The largest one, 18.7 ppm, is found for the complex G·Au₃(O₆; N₁ side).

In general, the data used in prerequisites iii–v (see also Table 1) provide an estimate of the hydrogen bonding interaction energy, E_{HB} . For the nonconventional N–H···Au hydrogen bonding studied here, such an estimation is not possible because of the presence of the anchor bond, which plays a key role in the H-bond formation. We can obtain an approximate upper bound for $|E_{\text{HB}}|$ by comparing the binding energies, say, of the planar complexes G·Au₃(O₆; N₁ side) and G·Au₃(O₆; N₇ side) (see Figure 3). They are characterized by the same Au–O anchor bond, but while G·Au₃(O₆; N₁ side) exhibits a nonconventional N–H···Au hydrogen bond, there is no such bond for G·Au₃(O₆; N₇ side). This gives the upper bound of $|E_{\text{HB}}| \leq 7.9$ kcal mol⁻¹. However, the anchor bond in G·Au₃(O₆; N₁ side) is much stronger than in the G·Au₃(O₆; N₇ side) (2.186 vs 2.239 Å), so that the upper bound given above should be lowered to

3–5 kcal mol⁻¹, which reasonably agrees with the upper bound found for similar nonconventional hydrogen bondings.¹⁴

To assess basis-set effects, two complexes, A·Au₃(N₃) and G·Au₃(O₆; N₁ side), respectively with the Au–N and Au–O anchor bonds, were further investigated at the higher computational level B3LYP/RECP (gold) ∪ 6-31++G(d,p) (DNA base). It is shown in Table 1 that the latter produces minor changes in nearly all the examined properties of these two complexes. Two other complexes, A·Au₄(N₃) and G·Au₄(O₆; N₁ side), with a T-shape four-gold cluster were also studied at this level (Figure 5). Their binding energies amount to 28.8 and 24.2 kcal mol⁻¹, respectively. The former possesses a very short (2.126 Å) Au–N anchor bond. Its N₉–H₉ bond is directed almost perpendicularly to the center of the diatomic bond Au₁₁–Au₁₂ forming two nonconventional H-bonds: N₉–H₉···Au₁₁ and N₉–H₉···Au₁₃, that results in a large $\Delta\nu(\text{N}_9\text{--H}_9)$ red shift of 275 cm⁻¹. In the latter complex, the Au–O anchor bond is rather short (2.157 Å), and two almost linear N–H···Au H-bonds are formed with guanine, viz., N₁–H₁···Au₁₁ with $\Delta\nu(\text{N}_1\text{--H}_1) = -172$ cm⁻¹ and N₂–H₂'···Au₁₂ with $\Delta\nu(\text{N}_2\text{--H}_2') = -191$ cm⁻¹.

In conclusion, we have shown that the bonding between DNA base and odd-size and even-size gold clusters, Au₃ and Au₄, occurs via the anchor Au–N or Au–O bonds. For all the possible binding sites of DNA, the structural, energetic, and spectroscopic features of the planar and, less stable nonplanar, base–Au_{3,4} complexes have been investigated. A novel type of nonconventional N–H···Au hydrogen bonding, which is formed in the most stable planar complexes between nucleic acid bases and triangle Au₃ and T-shape Au₄ gold clusters, has been identified. It is the formation of the anchor bond, either Au–N or Au–O, in the planar base–Au_{3,4} complexes that cooperatively, through charge redistribution, “catalyzes” one of the unanchored gold atoms to serve as a nonconventional proton acceptor and to form, via

its lone pair 5d orbital, a nonconventional hydrogen bond with the conventional proton donor of DNA base. In addition, under the assumption of a single-site base–Au_n binding, the reported affinities of DNA bases for Au₃ exhibit a fair correlation in magnitude and in relative order with the experimental findings. Note, however, that some reported anchoring sites of DNA bases are blocked by sugar residues for ssDNA as well as by the intramolecular hydrogen bonds for dsDNA, whereas the remaining sites are available for multisite bindings.

Acknowledgment. This work was partially supported by the Région Wallonne (RW. 115012). The computational facilities were provided by NIC (University of Liège) and by F.R.F.C. 9.4545.03 (FNRS, Belgium). E.S.K. gratefully thanks Profs. Lina M. Epstein, Camille Sandorfy, and George V. Yuhnevich for interesting discussions on the N–H...Au hydrogen bonds and valuable suggestions and F.R.F.C. 2.4562.03F for a fellowship.

References

- (1) (a) Tao, N. J.; de Rose, J. A.; Lindsay, S. M. *J. Phys. Chem.* **1993**, 97, 910. (b) Mirkin, C. A.; Letsinger, R. L.; Mucic, R. C.; Storhoff, J. J. *Nature* **1996**, 382, 607. (c) Alivisatos, A. P.; Johnsson, K. P.; Peng, X.; Wislon, T. E.; Loweth, C. J.; Bruchez, M. P., Jr.; Schultz, G. C. *Nature* **1996**, 382, 609. (d) Storhoff, J. J.; Mirkin, C. A. *Chem. Rev.* **1999**, 99, 1849. (e) Storhoff, J. J.; Lazarides, A. A.; Mucic, R. C.; Mirkin, C. A.; Letsinger, R. L.; Schatz, G. C. *J. Am. Chem. Soc.* **2000**, 122, 4640.
- (2) (a) Park, S.-J.; Lazarides, A. A.; Mirkin, C. A.; Letsinger, R. L. *Angew. Chem., Int. Ed.* **2001**, 40, 2909. (b) Niemeyer, C. M. *Angew. Chem., Int. Ed.* **2001**, 40, 4129. (c) Pirrung, M. C. *Angew. Chem., Int. Ed.* **2002**, 41, 1277. (d) Harnack, O.; Ford, W. E.; Yasuda, A.; Wessels, J. M. *Nano Lett.* **2002**, 2, 919.
- (3) (a) Parak, W. J.; Pellegrino, T.; Micheel, C. M.; Gerion, D.; Williams, S. C.; Alivisatos, A. P. *Nano Lett.* **2003**, 3, 33. (b) Alivisatos, A. P. *Nat. Biotechnol.* **2004**, 22, 47. (c) Daniel, M.-C.; Astruc, D. *Chem. Rev.* **2004**, 104, 293. (d) Seeman, N. C. *Nature* **2003**, 421, 427.
- (4) (a) Kimura-Suda, H.; Petrovykh, D. Y.; Tarlov, M. J.; Whitman, L. J. *J. Am. Chem. Soc.* **2003**, 125, 9014. (b) Demers, L. M.; Östblom, M.; Zhang, H.; Jang, N.-H.; Liedberg, B.; Mirkin, C. A. *J. Am. Chem. Soc.* **2002**, 124, 1128. (c) Storhoff, J. J.; Elghanian, R.; Mirkin, C. A.; Letsinger, R. L. *Langmuir* **2002**, 18, 6666. (d) Chen, Q.; Frankel, D. J.; Richardson, N. V. *Langmuir* **2002**, 18, 3219. (e) Giese, B.; McNaughton, D. J. *J. Phys. Chem. B* **2002**, 125, 1112. (f) Li, W.; Haiss, W.; Floate, S.; Nichols, R. *Langmuir* **1999**, 15, 4875. (g) Gourishankar, A.; Shukla, S.; Ganesh, K. N.; Sastry, M. *J. Am. Chem. Soc.* **2004**, 126, 13186. (h) Liu, Y.; Meyer-Zaika, W.; Franzka, S.; Schmid, G.; Tsoli, M.; Kuhn, H. *Angew. Chem., Int. Ed.* **2003**, 42, 2853.
- (5) (a) Roelfs, B.; Baumgärtel, H. *Ber. Bunsen-Ges. Phys. Chem.* **1995**, 99, 677. (b) Xiao, Y. J.; Chen, Y. F. *Spectrochim. Acta A* **1999**, 55, 1209. (c) Srinivasan, R.; Gopalan, P. *J. Phys. Chem.* **1993**, 97, 8770. (d) Camargo, A. P. M.; Baumgärtel, H.; Donner, C. *Phys. Chem. Chem. Phys.* **2003**, 5, 1657 and references therein.
- (6) Wells, D. H. Jr.; Delgass, W. N.; Thomson, K. T. *J. Catal.* **2004**, 225, 69 and references therein.
- (7) Ross, R. B.; Powers, J. M.; Atashroo, T.; Ermler, W. C.; LaJohn, L. A.; Christiansen, P. A. *J. Chem. Phys.* **1990**, 93, 6654.
- (8) (a) Remacle, F.; Kryachko, E. S. *Adv. Quantum Chem.* **2004**, 47, 423. (b) Remacle, F.; Kryachko, E. S. *J. Chem. Phys.* **2005**, 122, 044304.
- (9) Frisch, M. J.; Trucks, G. W.; Schlegel, H. B.; Scuseria, G. E.; Robb, M. A.; Cheeseman, J. R.; Zakrzewski, V. G.; Montgomery, J. A.; Stratmann, R. E.; Burant, J. C.; Dapprich, S.; Millan, J. M.; Daniels, A. D.; Kudin, K. N.; Strain, M. C.; Farkas, O.; Tomasi, J.; Barone, V.; Cossi, M.; Cammi, R.; Mennucci, B.; Pomelli, C.; Adamo, C.; Clifford, S.; Ochterski, J.; Peterson, G. A.; Ayala, P. Y.; Cui, Q.; Morokuma, K.; Malick, D. K.; Rabuck, A. D.; Raghavachari, K.; Foresman, J. B.; Cioslowski, J.; Ortiz, J. V.; Stefanov, B. B.; Liu, G.; Liashenko, A.; Piskorz, P.; Komaromi, I.; Gomperts, R.; Martin, R. L.; Fox, D. J.; Keith, T.; Al-Laham, M. A.; Peng, C. Y.; Nanayakkara, A.; Gonzalez, C.; Challacombe, M.; Gill, P. M. W.; Johnson, B. G.; Chen, W.; Wong, M. W.; Andres, J. L.; Head-Gordon, M.; Replogle, E. S.; Pople, J. A. *GAUSSIAN 03* (revision A.1), Gaussian, Inc.: Pittsburgh, PA, 2003.
- (10) (a) Pimentel, C. G.; McClellan, A. L. *The Hydrogen Bond*; W. H. Freeman: San Francisco, 1960. (b) *The Hydrogen Bond. Recent Developments in Theory and Experiments*, Schuster, P.; Zundel, G.; Sandorfy, C., Eds.; North-Holland: Amsterdam, 1976. (c) Jeffrey, G. A.; Saenger, W. *Hydrogen Bonding in Biological Structures*; Springer: Berlin, 1991. (d) Scheiner, S. *Hydrogen Bonding. A Theoretical Perspective*; Oxford University Press: Oxford, 1997. (e) Desiraju, G. R.; Steiner, T. *The Weak Hydrogen Bond in Structural Chemistry and Biology*; Oxford University Press: Oxford, 1999. (f) Steiner, T. *Angew. Chem. Int. Ed.* **2002**, 41, 48.
- (11) (a) Hinton, J. F.; Wolinski, K. in *Theoretical Treatments of Hydrogen Bonding*, Hadži, D., Ed.; Wiley: Chichester, 1997; p 75. (b) Becker, E. D. In *Encyclopedia of Nuclear Magnetic Resonance*; Grant, D. M.; Harris, R. K., Eds.; Wiley: New York, 1996; p 2409. (c) Kar, T.; Scheiner, S. *J. Phys. Chem. A* **2004**, 108, 9161 and references therein.
- (12) (a) Epstein, L. M.; Shubina, E. S. *Coord. Chem. Rev.* **2002**, 231, 165. (b) Brammer, L. *Dalton Trans.* **2003**, 3145 and references therein.
- (13) (a) Chandra, A. K.; Nguyen, M. T.; Uchimar, T.; Zeegers-Huyskens, T. *J. Phys. Chem. A* **1999**, 103, 8853. (b) Kryachko, E. S.; Nguyen, M. T.; Zeegers-Huyskens, T. *J. Phys. Chem. A* **2001**, 105, 1288, 1934.
- (14) Kryachko, E. S.; Remacle, F. *Chem. Phys. Lett.* **2005**, 404, 142.

NL050194M